International Journal of Electronics Communication and Computer Engineering
Volume 3, Issue 4, ISSN (Online): 2249–071X, ISSN (Print): 2278–4209

An Accurate AOS Scheme for Multiplicative Noise Removal Model Based on TV Approach

Asmat Ullah **Mushtaq Ahmad Khan**

***Abstract*- This paper presents an efficient Additive Operator Splitting (AOS) scheme for solution of non-linear PDEs arisen from minimization of multiplicative noise removal model [12]. It is a stable, fast and easy method to implement, avoids the complicated governing equations and appear to converge in fewer iterations. This method successively de-noised the images. Furthermore, fixed point and semi-implicit schemes are also implemented to yield our desired results. Experiments demonstrate that, under typical accuracy requirements, AOS scheme is more efficient than the widely used iterative schemes of fixed point and semi-implicit.**

***Keywords*- Synthetic Aperture Radar (SAR), Total Variation (TV), AOS (Additive Operator Splitting), MAP (Maximum A Posteriori).**

I. INTRODUCTION

Image de-noising has been drawn a greatly attention recently. It is an inverse problem encountered in a wide variety of image processing fields including remote sensing, medical and astronomical applications [8, 18, 12]. In this paper, we focus on multiplicative noise removal problems. It is one of the more complex image noise. It is signal independent, non-Gaussian and spatially dependent. It appears in various image processing applications e.g. in Synthetic Aperture Radar (SAR), Utrasound imaging or in connection with blur in electronic microscopy, single particle emission computed tomography (SPECT) and Positron Emission Tomogra phy (PET). Many approaches have been proposed to tackle this problem. Among the famous ones are wavelets approaches, stochastic approaches, and variational approaches which is presented by Rudin, Osher and Fatemi (ROF) [14], it become evident that the variational approaches to the image denoising problem can yield often excellent results. In the literature, there exist several variational approaches devoted to multiplicative noise removal problems: $z = \Phi\eta$. The first TV-based multiplicative noise removal model was introduced by Rudin etal(RLO-model) [13] which used a constrained optimization approach with two Lagrange multipliers.

Multiplicative de-noising model (AA-model) with a fitting term obtained from a MAP (Maximum a Posteriori) was presented by Aubert and Aujol [19, 1]. Shi and Osher [14, 12] adopted the data term of the AA-model and replace the regularizer $TV(\Phi)$ by $TV(log\Phi)$ and letting $w = log\Phi$, they derived the strictly convex TV model (SOmodel) [5]. Similarly with SO-model, Bioucas and Figueiredo converted the multiplicative model into an additive one by taking logarithms and introduced Bayesian type variational model[12]. Steidl and Teuber [12, 20] presented a variational model consisting of the 1-divergence as data fitting term and the TV-seminorm as regularizer. A variational model involving curvelet coefficients for cleaning multiplicative Gamma noise was introduced in [12].

Most numerical schemes are based on the simplest finite difference discretization by means of a so called explicit or Euler-forward scheme. This scheme requires very small time steps in order to be stable. Hence the whole procedure is rather timeconsuming. In the present paper, we are going to address this problem. We present a novel type of separable scheme which do not suffer from any time step size restriction since all stability relevant terms are discretized in an implicit manner. The goal of this paper, is to apply Additive Operator Splitting (AOS) Scheme and to compare its results with fixed point and semi-implicit schemes [2, 11, 9, 3].

II. VARIATIONAL MODEL

According to [12] by applying the Total Variational (TV) approach, a functional well-adapted to the removing of multiplicative noise is given by:

$$\min_{\Phi}\left\{\int_{\Omega}\left(log\Phi+\frac{z}{\Phi}\right)dx+\gamma_1\int_{\Omega}|D\Phi|+\gamma_2\int_{\Omega}\frac{|D\Phi|}{\Phi}\right\} \tag{1}$$

where, the first term is the image fidelity term which measures the violation of the relation between Φ and the observation z. The last two terms are the regularization terms, where $\gamma 1$, $\gamma 2$ are regularization parameters. The formal Euler-Lagrange equation [12] for any solution of functional (1) is as follows.

$$\begin{aligned} &-\left(\frac{\gamma_1\Phi+\gamma_2}{\Phi}\right)\nabla\cdot\left(\frac{\nabla\Phi}{\sqrt{|\nabla\Phi|^2+\epsilon}}\right)+\frac{\Phi-z}{\Phi^2}=0 \quad \text{in } \Omega \\ &\frac{\partial\Phi}{\partial\vec{n}}=0 \quad \text{on } \partial\Omega \end{aligned} \tag{2}$$

since $\Phi > 0$, then the Euler-Lagrange equation of minimizing can be rewritten equivalently as

$$\begin{aligned} &-\nabla\cdot\left(\frac{\nabla\Phi}{\sqrt{|\nabla\Phi|^2+\epsilon}}\right)+\frac{\Phi-z}{\Phi(\gamma_1\Phi+\gamma_2)}=0 \quad \text{in } \Omega \\ &\frac{\partial\Phi}{\partial\vec{n}}=0 \quad \text{on } \partial\Omega \end{aligned} \tag{3}$$

International Journal of Electronics Communication and Computer Engineering
Volume 3, Issue 4, ISSN (Online): 2249–071X, ISSN (Print): 2278–4209

Let $\tilde{\lambda} = \tilde{\lambda}(\Phi) = \frac{1}{\Phi(\gamma_1\Phi + \gamma_2)}$. Then equation (3) can be rewritten as

$$-\nabla \cdot \left(\frac{\nabla\Phi}{\sqrt{|\nabla\Phi|^2 + \epsilon}}\right) + \tilde{\lambda}(\Phi - z) = 0, \quad \text{in } \partial\Omega \tag{4}$$

with the Neumann adiabatic condition along the boundary of the image domain. Notice that $\tilde{\lambda} > 0$, since $\Phi > 0$. Equation (4) can be expressed in operator notation

$$L(\phi)\Phi = \tilde{\lambda}(\Phi)z \tag{5}$$

where $L(\Phi)$ is the linear diffusion operator whose action on a function χ is given by:

$$L(\Phi)\chi = -\nabla \cdot \left(\frac{\nabla\chi}{\sqrt{|\nabla\Phi|^2 + \epsilon}}\right) + \tilde{\lambda}(\Phi)\chi \tag{6}$$

The fixed point iteration is then

$$L(\Phi^{(n)})\Phi^{(n+1)} = \tilde{\lambda}(\Phi^{(n)})z, \; n = 0, 1, 2, \cdots \tag{7}$$

Finite difference method [10, 6, 4], is used commonly for discretization of Partial ifferential equation (PDE). Equation (5) can be approximately computed by the first order accurate finite difference schemes described as follows [13, 12],

$$D_x^{\pm} = \pm[\Phi_{i\pm1,j} - \Phi_{i,j}], D_y^{\pm} = \pm[\Phi_{i,j\pm1} - \Phi_{i,j}] \tag{8}$$

$$|D_x(\Phi_{i,j})|_\epsilon = \sqrt{D_x^+(\Phi_{i,j})^2 + (m[D_y^+(\Phi_{i,j}), D_y^-(\Phi_{i,j})])^2 + \epsilon} \tag{9}$$

$$|D_y(\Phi_{i,j})|_\epsilon = \sqrt{D_y^+(\Phi_{i,j})^2 + (m[D_x^+(\Phi_{i,j}), D_x^-(\Phi_{i,j})])^2 + \epsilon} \tag{10}$$

where $m(a, b) = (sign(a)+sign(b))/2$, $min(|a|, |b|)$. Here, we denote the space step size by $h = 1$, $\epsilon > 0$. These schemes yield approximate form of equation (6) :

$$L(\Phi)\chi \approx \left(D_x^-\left(\frac{D_x^+\chi}{|D_x\Phi|_\epsilon}\right) + \left(D_y^-\left(\frac{D_y^+\chi}{|D_y\Phi|_\epsilon}\right) + \tilde{\lambda}(\Phi)\chi\right.\right. \tag{11}$$

The matrix operators L, are symmetric and positive definite and sparse. Following experimental results will illustrate the performance of the numerical scheme [7].

III. Numerical Methods

Explicitly time marching methods have been applied for solving TV-image models [16], due to their simplicity but as it is conditionally stable. Therefore, we use the Semi-Implicit (SI) scheme and Additive Operator Splitting (AOS) which are unconditionally stable. To solve equation (4) with an artificial time step Δt i.e the following problem:

$$\Phi_t = -\nabla \cdot \left(\frac{\nabla\Phi}{\sqrt{|\nabla\Phi|^2 + \epsilon}}\right) + \tilde{\lambda}\left(\Phi - z\right) \quad in \quad \Omega \tag{12}$$

with the Neumann adiabatic condition along the boundary of the image domain. Where $\tilde{\lambda} = \tilde{\lambda}(\Phi) = \frac{1}{\Phi\left(\gamma_1\Phi + \gamma_2\right)}$.

The grid-point (i, j) is located at

$$(x_i, y_j) = \left(a + \frac{(2i-1)h}{2}, c + \frac{(2j-1)k}{2}\right)$$

Where

$$1 \le i \le m_1, 1 \le j \le m_2$$

The value of z at each grid (i, j) is denoted by $z(i,j)$ where as $h = \frac{b-a}{m_1}$, $k = \frac{d-c}{m_2}$ are the grid spacings in the x, y-directions.

A. Semi-Implicit Scheme

Refer to [3, 17], at time $tn = n\Delta t$, denote $\Phi n\ i,j = \Phi(tn, xi, yj)$ an approximation of $\Phi(t, x, y)$ and using equation (4–12) we obtain the following linearized equation through semi-implicitness is given as:

$$\frac{\Phi_{i,j}^{n+1} - \Phi_{i,j}^n}{\Delta t} = D_x^-\left(\frac{D_x^+\Phi_{i,j}^{n+1}}{\sqrt{\left(D_x^+\Phi_{i,j}^n/h\right)^2 + \left(\Phi_{i,j+1}^n - \Phi_{i,j-1}^n/2k\right)^2}}\right) + D_y^-\left(\frac{D_y^+\Phi_{i,j}^{n+1}}{\sqrt{\left(\left(\Phi_{i+1,j}^n - \Phi_{i-1,j}^n/2h\right)^2 + \left(D_y^+\Phi_{i,j}^n/k\right)^2\right)}}\right) + \tilde{\lambda}\left(z_{i,j} - \Phi_{i,j}^{n+1}\right) \tag{13}$$

Denoting the coefficients of $\Phi_{i+1,j}^{n+1}, \Phi_{i-1,j}^{n+1}, \Phi_{i,j+1}^{n+1}, \Phi_{i,j-1}^{n+1}$, by A_1, A_2, A_3, A_4, respectively, we get the following system of linear equations

$$[1 + \Delta t\tilde{\lambda} + A_1 + A_2 + A_3 + A_4]\Phi_{i,j}^{n+1} = \Phi_{i,j}^n + \Delta t[A_1\Phi_{i+1,j}^{n+1} + A_2\Phi_{i-1,j}^{n+1} + A_3\Phi_{i,j+1}^{n+1} + A_4\Phi_{i,j-1}^{n+1}] + \Delta t\tilde{\lambda}z_{i,j} \tag{14}$$

which may be solved by an iterative method as a direct solution can be expensive for images of large size.

B. Additive Operator Splitting Scheme

It is already stated that semi-implicit scheme is unconditionally stable but it is can allow large time steps. Its main drawback is the computational cost of the associated linear systems for large images. Hence, we need an iterative method which is unconditionally stable, time efficient and easy to implement to solve the PDEs. So we introduce the AOS scheme [3, 15], which provides an equally accurate and yet more efficient SI-scheme by splitting the two dimensional spatial operator into two separate 1- dimensional space discretizations and then applying 1-dimensional SI-scheme in turns. Then two tridiagonl systems are solved per iteration than a band five system. Following equation (12) we have

International Journal of Electronics Communication and Computer Engineering
Volume 3, Issue 4, ISSN (Online): 2249–071X, ISSN (Print): 2278–4209

$$\Phi_t = -\tilde{\mu}\,\nabla\cdot\left(\frac{\nabla\Phi}{\sqrt{|\nabla\Phi|^2+\epsilon}}\right)+\Phi-z \quad in \quad \Omega \quad (15)$$

with the Neumann adiabatic condition along the boundary of the image domain. Where $\tilde{\mu}=\tilde{\mu}=(\Phi)=\Phi(\gamma_1\Phi+\gamma_2)$. Consider (15) in the form

$$\frac{\Phi_i^{n+1}-\Phi_i^n}{\partial t} = -\tilde{\mu}\,\nabla\cdot\left(Q\nabla\Phi\right)+\Phi-z$$
$$= -\tilde{\mu}(\partial_x(Q\partial_x\Phi)+\partial_y(Q\partial_y\Phi))+\Phi_i^{n+1}-z_i \quad (16)$$

where $Q=\frac{1}{\sqrt{|\nabla\phi|^2+\epsilon}}$

$$\frac{\Phi_i^{n+1}-\Phi_i^n}{\partial t} =$$
$$-\tilde{\mu}\left[\left(\frac{Q_i^n+Q_{i+1}^n}{2}\right)\left(\Phi_{i+1}^{n+1}-\Phi_i^n\right)\right.$$
$$\left.-\left(\frac{Q_i^n+Q_{i-1}^n}{2}\right)\left(\Phi_i^{n+1}-\Phi_{i-1}^{n+1}\right)\right]$$
$$+\Phi_i^{n+1}-z_i \quad (17)$$

$$\Rightarrow \Phi_i^{n+1}-\Phi_i^n = -\tilde{\mu}\,\partial t\left[\left(\frac{Q_i^n+Q_{i+1}^n}{2}\right)\right.$$
$$\left(\Phi_{i+1}^{n+1}-\Phi_i^n\right)$$
$$\left.-\left(\frac{Q_i^n+Q_{i-1}^n}{2}\right)\left(\Phi_i^{n+1}-\Phi_{i-1}^{n+1}\right)\right]$$
$$+\partial t\left(\Phi_i^{n+1}-z_i\right) \quad (18)$$

$$\Rightarrow \Phi_i^{n+1} = \Phi_i^n-\tilde{\mu}\,\partial t\left[\left(\frac{Q_i^n+Q_{i+1}^n}{2}\right)\Phi_{i+1}^{n+1}-\right.$$
$$\left(\frac{Q_{i-1}^n+2Q_i^n+Q_{i+1}^n}{2}\right)\Phi_i^n$$
$$\left.+\left(\frac{Q_i^n+Q_{i-1}^n}{2}\right)\Phi^{n+1}\right]+\partial t\Phi_i^{n+1}-\partial t z_i \quad (19)$$

i.e

$$\Phi_i^{n+1} = \Phi_i^n-\tilde{\mu}\,\partial t\left[c_1\Phi_{i+1}^{n+1}-c_2\Phi_i^{n+1}+\right.$$
$$\left.c_3\Phi_{i-1}^{n+1}\right]+$$
$$\partial t\Phi_i^{n+1}-\partial t z_i \quad (20)$$

where, $c_1=\frac{Q_i^n+Q_{i+1}^n}{2}$, $c_2=\frac{Q_{i-1}^n+2Q_i^n+Q_{i+1}^n}{2}$, $c_3=\frac{Q_i^n+Q_{i-1}^n}{2}$

After we solve the system of equations (17) in the x-direction, we then solve a similar system in the y-direction before averaging the two solutions. In matrix notation the process can be written as

$$\left(I-2\partial t A_l\left(\Phi^n\right)\right)\Phi_l^{n+1}=z^n, \quad \text{for} \quad l=1,2$$
$$\text{and} \quad \Phi^{n+1}=\frac{1}{2}\sum_{l=1}^{2}\Phi_l^{n+1} \quad (21)$$

where I is the identity matrix, and Al *forl* = 1, 2. are tridiagonal matrices derived from (18).

IV. Experimental Results

In this paper, experiments are carried out on gray scale images of different sizes (pixels) and ranges from [0 127] to [0 2047] with multiplicative noise. Experimental results are given to demonstrate the performance of AOS and comparison is made with numerical schemes of semi-implicit, fixed point. Figure1 shows test images for de-noising namely Problem1, Problem2, Problem3, Problem4, Problem5, and Problem6. The de-noised images are shown in figure2, figure3, figure4, figure5, figure6 and figure7 for visual comparison. Figure2 consists of problem1 in which artificial speckle is added, is de-noised by semi-implicit, fixed Point and additive operator splitting schemes by choosing $\gamma1$ = 10, $\gamma2$ = .007. Figure3 shows problem2 includes the lena famous natural image, in this case the restoration of image is made by applying semi-implicit, fixed point iterative and additive operator splitting schemes with $\gamma1$ = .005, $\gamma2$ = .0005. Figure4 involves problem3, which is restored by semi-implicit, fixed point, additive operator splitting scheme, with $\gamma1$ = .01, $\gamma2$ = .0001. Figure5 shows problem4, which is restored by semi-implicit, fixed Point, additive operator splitting scheme, with $\gamma1$ = 15, $\gamma2$ = .003. Figure6 contains problem5 which shows the real-time ultrasound image of an human eye corrupted by speckle, is restored by semi-implicit, fixed point, additive operator splitting scheme, with $\gamma1$ = .003, $\gamma2$ = .0009. Here in this case more better result is needed which will be address in our future work by applying multi-grid algorithm. Although by comparing the results of AOS with semi-implicit and fixed-point it can be seen that AOS is effective and efficient than the other two iterative schemes. Figure7 shows problem6 corrupted by multiplicative noise naturally, is restored by semi-implicit, fixed Point, additive operator splitting scheme, with $\gamma1$ = .001, $\gamma2$ = .091. In this case it is concluded that AOS results are much better and fast than the iterative schemes of semi-implicit and fixed-point. By visual comparison better performance of AOS can be seen over semi-implicit and fixed-point iterative schemes in all artificial and natural images. In addition, from table1 one can conclude that AOS is more efficient and effective. Furthermore, we gave the speed comparison of the three schemes which includes the number of iterations (It.) and the CPU time for the images of different sizes. Following abbreviations may be helpful for reading the given table which is given as under: SIM: Semi-Implicit Scheme, FPIS: Fixed Point Iteration Scheme, AOS: Additive Operator Splitting Scheme.

International Journal of Electronics Communication and Computer Engineering
Volume 3, Issue 4, ISSN (Online): 2249–071X, ISSN (Print): 2278–4209

C. Test Images for De-noising

Following are the test images which will be used for de-noising throughout in this work, which are assigned names as Problem1, Problem2, Problem3, Problem4, Problem5 and Problem6.

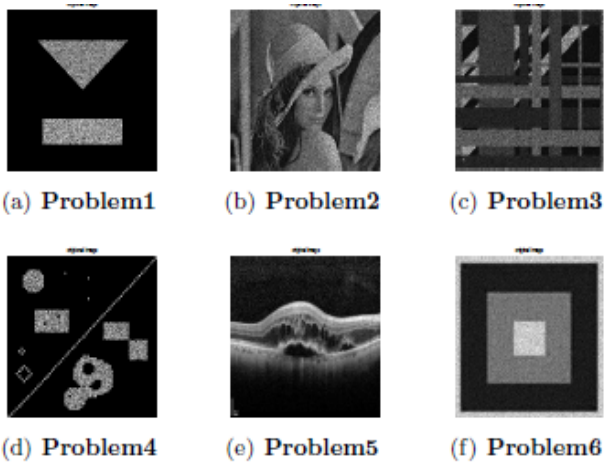

(a) **Problem1** (b) **Problem2** (c) **Problem3**

(d) **Problem4** (e) **Problem5** (f) **Problem6**

Fig.1. Test images for de-noising

(a) It.=55,SIM (b) It.=105,FPIM (c) It.=17,AOS

Figure.2. Problem1 (2562) de-noised image by semi implicit, fixed point, additive operator splitting schemes with number of iterations=55, 105, 17 by choosing γ_1 = 10, γ_2 = .007.

(a) It.=26,SIM (b) It.=70,FPIM (c) It.=5,AO

Fig.3. Problem2 (2562) de-noised image by semi implicit, fixed point, additive operator splitting schemes with number of iterations=26, 70, 5 by choosing γ_1 = .003, γ_2 = .0005.

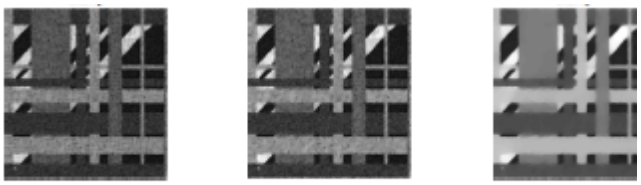

(a) It.=34,SIM (b) It.=30,FPM (c) It.=5,AO

Fig.4. Problem3 (2562) de-noised image by semi implicit, fixed point, additive operator splitting schemes with number of iterations=34, 30, 5 by choosing γ_1 = .001, γ_2 = .01.

(a) It.=62,SIM (b) It.=20,FPIM (c) It.=10, AOS

Fig.5. Problem4 (2562) de-noised image by semi implicit, fixed point, additive operator splitting schemes with number of iterations=62, 20, 10, by choosing γ_1 = 15, γ_2 = .003

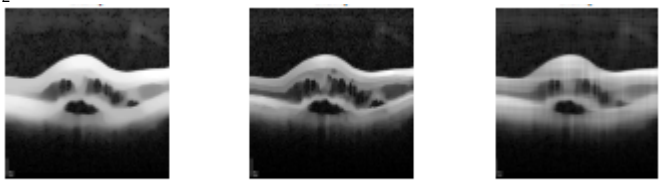

(a) It.=15, SIM (b) It.=100,FPIM (c) It.=8,AOS

Fig.6. Problem5 (2562) de-noised image by semi implicit, fixed point, additive operator splitting schemes with number of iterations=15, 100, 8, by choosing γ_1 = .003, γ_2 = .0009.

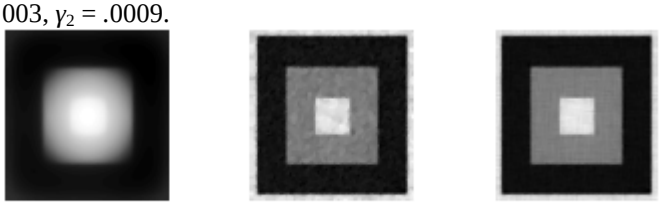

(a) It.=7, SIM (b) It.=40,FPIM (c) It.=11,AOS

Fig.7. Problem6 (2562) de-noised image by semi implicit, fixed point, additive operator splitting schemes with number of iterations=7, 40, 11, by choosing γ_1 = .001, γ_2 = .091

Pb	size	SIM		FPIS		AOS	
		It.	cpu	It.	cpu	It.	cpu
Pb1	128^2	25	3	70	20	15	3
	256^2	55	15	105	31	17	5
	512^2	50	75	100	85	16	9
	1024^2	59	400	109	165	19	78
	2048^2	71	586	127	730	22	195
Pb3	128^2	11	2	28	10	7	1
	256^2	34	13	30	154	5	3
	512^2	19	87	55	824	8	14
	1024^2	25	735	75	997	10	35
	2048^2	31	2031	87	2528	10	130

Table 1: Comparison of semi-implicit, fixed point iteration, additive operator splitting schemes for multiplicative noise images of Problem1 (1282 −20482) and Problem3 (1282 − 20482) with cpu-time and number of iterations

V. Peak Signal-to-Noise Ratio (PSNR)

We measure the quality of the restored image by the peak signal-to-noise ratio (*PSNR*) defined by

$$PSNR = 10\ log_{10}\left[\frac{(m_1 \times m_2)max(\Phi)^2}{\|z-\Phi\|^2}\right]$$

where z is the original image, Φ is the restored image and $m1 \times m2$ is the size of the image.

Problem	Size	SIM	FPIS	AOS
		PSNR	PSNR	PSNR
Problem1	256^2	23.05	17.54	23.37
Problem3	256^2	34.03	19.23	34.78

Table 2: It shows the Peak Signal-to-Noise Ratio (*PSNR*) results by semi-implicit, fixed point, additive operator splitting schemes on gray level image of problem1 and problem3. From the table, we can see that the PSNR of the image restored by using AOS is more than those restored by using the other schemes.

VI. Conclusion

In this paper, accurate additive operator splitting scheme for multiplicative noise/speckle removal is presented. Comparing the experimental results of two numerical schemes fixed point and semi-implicit with AOS, it is found that Additive Operator Splitting scheme is simple, reliable and more efficient than iterative schemes of fixed point and semiimplicit. Future work is needed to apply multi-grid algorithm to yield more effective and better results as the technique has the advantage of speed of computation and has a large potential in real-time ultrasound imaging enhancement. It may also offer a particular advantage for processing very larger images. Furthermore, it is intended to apply Additive Multiplicative Operator Splitting (AMOS) scheme for PDEs arisen from minimization of variational models.

References

[1] G. Aubert and J. F. Aujol, *A variational approach to removing multiplicative noise*, SIAM Journal on Applied Mathematics 68 (2008), no. 4, 925–946.

[2] G. Aubert and P. Kornprobst, *Mathematical problems in image processing of applied athematical sciences*, Springer, Berlin, Germany 147 (2002).

[3] N. Badshah and K. Chen, *Multigrid method for the chan-vese model in variational segmentation*, Communications in Computational Physics 4 (2008), no. 2, 294–316.

[4] N. Badshah and K. Chen, *On two multi-grid algorithms for modelling variational multiphase image segmentation*, IEEE transactions on image Processing 18 (2009), no. 5, 1097–1106.

[5] C.B. Burkhardt, *Speckle in ultrasound b-mode scans*, IEEE Trans. Ultrasonic, 25 (1978), no. 1, 1–6.

[6] Y. Liping C. Sheng, Y. Xin and S. Kun, *Total variation based speckle reduction using multigrid algorithm for ultrasound images*, Springer-Verlag Berlin Heidelberg 36 (2005), no. 17, 245–252.

[7] S. Dangeti, *Denoising techniques-a comparison*, Master's thesis, B.E., Andhra University College of Engineering, Visakhapatnam, India, 2003.

[8] X. Zeng F. Tian Z. Li G, Liu and K. Chaibou, *Speckle reduction by adaptive window anisotropic diffusion*, signal processing 89 (2009), no. 11, 233–243.

[9] J. W. Goodman, *Some fundamental properties of speckle*, Journal of Opt. Soc. Am. 66 (1976), no. 6, 1145–1150.

[10] D. C. Munson Jr and R. L. Visentin, *A signal processing view of strip-mapping synthetic aperture radar*, IEEE Transactions on accoustics, speech, and signal processing, 37 (1989), no. 12, 2131–2147.

[11] R. Kikinis K. Krissian, C. F. Westin and K. G. Vosburgh, *Oriented speckle reducing anisotropic diffusion*, IEEE Transactions on image processing 16 (2007), no. 5, 142–155. [12] L. Xiao L. Huang and Z. H. Wei, *Multiplicative noise removal via a novel variational model*, EURASIP Journal on image and video processing 1135 (2010), no. 250768, 768–782.

[13] P. L. Lions L. I. Rudin and S. Osher, *Multiplicative denoising and deblurring theory and algorithms, in geometric ,level set methods in imaging, vision, and graphics, s. osher and n. paragios, ed.*, Springer, Berlin, Germany, (2003), 103–120.

[14] S. Osher L. I. Rudin and E. Fatemi, *Non-linear total variation based noise removal algorithms*, Physica D 60 (1992), 259–268.

[15] P. Lin R. Glowinski and X. B. Pan, *An operator-splitting method for a liquid crystal model,*, comp. Phys. Comm. 152 (2003), no. 152, 242–252.

[16] M.M. Crawford S. T. Acton, A.C. Bovik, *Anisotropic diffusion processing for image segmentation*, Proc. IEEE Int. Conf. Image Processing (ICIP-94),Austin 3 (1994), no. 478-482.

[17] J. Shen, *On the foundation of vision modeling: I. weber's law and weberized tv restoration*, Physica D 175 (2003), no. 3-4, 241–251.

[18] J. Shi and S. Osher, *A nonlinear inverse scale space method for a convex multiplicative noise model,*, SIAM Journal on imaging sciences, 1 (2008), no. 3, 294–321.

[19] M. Bertalmio G. Sapiro V. Vaselles, C. Ballester and J. Verera, *Filling in by joing interpolation of vector fields and grey levels*, IMA Technical Report, university of Minnesota 69 (2002), no. 7, 131–147.

[20] M. K. Ng. Y. M. Huang and Y. W.Wen, *A new total variation method for multiplicative noise removal,*, SIAM Journal on imaging sciences, 2 (2009), no. 1, 22–40. Author's Profiles:

Author's Profile

Asmat Ullah
Lecturer
Department of Basic Sciences,
UET Peshawar, Pakistan.
asmatullah75@gmail.com

Mushtaq Ahmad Khan
Lecturer
Department of Basic Sciences,
UET Peshawar, Pakistan. 7
mushtaq@nwfpuet.edu.pk